Viscoelastic behavior of 80In15Pb5Ag and 50Sn50Pb alloys: Experiment and modeling

L. K. Edwards
Edwards Consulting, 3501 Oriole Court NE, Cedar Rapids, Iowa 52402

R. S. Lakes[a)]
Department of Engineering Physics, Engineering Mechanics Program, University of Wisconsin–Madison, 147 Engineering Research Building, 1500 Engineering Drive, Madison, Wisconsin 53706-1687

W. A. Nixon
Department of Civil and Environmental Engineering and Institute of Hydraulic Research, University of Iowa, Iowa City, Iowa 52242

(Received 8 July 1999; accepted for publication 14 October 1999)

Dynamic and creep behavior of 80In15Pb5Ag and 50Sn50Pb were studied isothermally over nine decades of time and frequency. 80In15Pb5Ag was examined at −6, 21, and 50 °C, and 50Sn50Pb was examined at 21 °C. Viscoelastic behavior was observed at strains less than 10^{-5} as a function of temperature and time/frequency. At the small strain used in the study, the alloys exhibit linear viscoelasticity rather than the viscoplasticity observed at larger strain. Viscoelasticity was subject to constitutive modeling. The creep followed a superposition of a stretched exponential and a power law in time, and an Arrhenius form in temperature. Behavior was thermorheologically simple over at least nine decades of true time and frequency. © *2000 American Institute of Physics.*
[S0021-8979(00)02203-9]

I. INTRODUCTION

Viscoelasticity in metals is of interest in the context of fundamental understanding of microscopic processes and in the context of current or potential applications. Alloys of low melting point are used in soldering. Such alloys can exhibit substantial viscoelasticity. The performance of these solders in electronic devices is related to their viscoelastic behavior (creep); damping can be important under vibratory forces. Flow or cracking of a solder joint can lead to failure of the device containing that joint. The most common solders used in electronic packaging are tin/lead based; these have been studied in detail over the past two decades. Recently, there has been interest in using solders other than tin/lead in microelectronic packaging. Some such solders, such as eutectic In–Sn, tend to exhibit more creep than Pb–Sn.

Substantial viscoelastic response in metals is commonly but not exclusively associated with high homologous temperature $T_H = T/T_{\text{melting}} > 0.5$, with T as the absolute temperature. Most solders are at high homologous temperature at room temperature. Viscoelasticity in metals at high homologous temperature is often dominated by ''high-temperature background.'' Nowick and Berry[1] discussed the high-temperature background in their classic reference on an elastic behavior, in which they comment (i) that its magnitude is highly structure sensitive in that it is smaller in single crystals than in polycrystals, (ii) that its magnitude is smaller in coarse-grained polycrystals than in fine-grained polycrystals, (iii) it is enhanced in deformed and partially recovered or polygonized samples, and (iv) it is reduced by annealing treatments at successively higher temperatures. High-temperature background is thought to be caused by a combination of thermally activated dislocation mechanisms.

The purpose of this research was to study the viscoelastic behavior of several solders as a function of time, temperature, and frequency, and to model the results by a constitutive equation. Dynamic (sinusoidal) and creep behavior of 80In15Pb5Ag was measured isothermally at −6, 21, and 50 °C. In addition, the dynamic and creep behavior of 50Sn50Pb was measured at 21 °C.

II. MATERIALS AND METHODS

The 80In15Pb5Ag alloy was solder wire from Indium Corporation of America; it was of diameter 1.21 mm and length 22.6 mm. The 50Sn50Pb alloy was solder wire of diameter 1.91 mm and of length 18.9 mm. Specimens were cut to length with a diamond saw.

The instrument used is capable of measuring the viscoelastic properties of a solid material over more than ten decades of time and frequency. A detailed description of the instrument can be found in Brodt *et al.*[2] A schematic diagram of the test instrument is shown in Fig. 1. Torque is applied electromagnetically to a cylindrical specimen fixed at one end. Specimen deformation is determined via a laser beam reflected from the rotating end onto a split diode detector.

Several improvements in the test apparatus were made to facilitate this investigation. The signal-to-noise ratio was improved by modifying the light detector amplifier circuit. Plexiglas shielding was added to reduce low-frequency noise introduced by air currents. The body of the apparatus is a brass cylinder, 1 cm thick, which shields electrostatic fields.

[a)]Author to whom correspondence should be addressed; electronic mail: lakes@engr.wisc.edu

 © 2000 American Institute of Physics

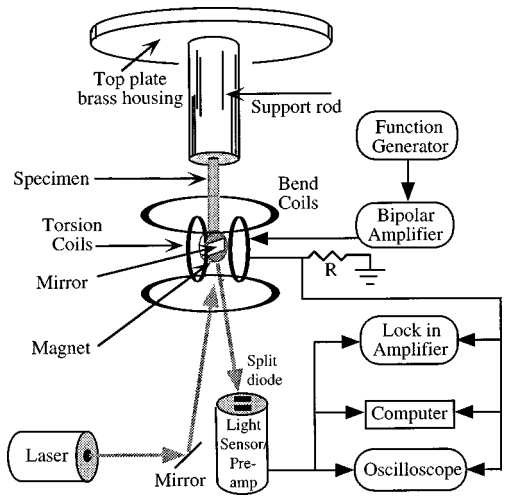

FIG. 1. Schematic diagram of the apparatus, adapted from Refs. 2, 17.

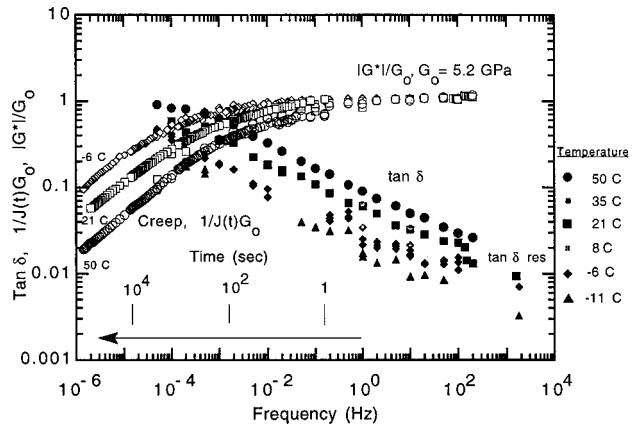

FIG. 2. Stiffness and tan δ vs frequency and temperature for 80In15Pb5Ag (shear modulus, $G_0 = 5.2$ GPa at 1 Hz, 21 °C).

High permeability mu-metal shielding was added to eliminate parasitic torque due to static and quasistatic magnetic fields. Heating and cooling capacity was added so that viscoelastic measurements could be made at other than ambient temperature. A refrigerated probe with temperature control (FTS systems) was inserted into the apparatus for studies below ambient temperature, and a heated probe was used above ambient. Noise due to convection currents during cooling limited most tests to −6 °C; some tests were done at −11 °C.

Torque and angular displacement were measured in this experiment. Stress and strain were inferred via the solution of a boundary value problem for the specimen geometry in question. For dynamic torsional experiments, an exact solution is available for the boundary value problem of a solid rod of circular cross section.[3] For bending, quasi-static experiments can be analyzed approximately using the corresponding exact analytical solution for static bending. At resonances, damping was calculated using the method of resonant half widths, described below. Surface strain in dynamic experiments was less than 10^{-5}. Linearity was studied by examination of the shape of the Lissajous figures of the dynamic stress-strain behavior (they are elliptic in a linear material) and by repeated experiments at different load level.

Creep experiments were conducted by using an electrical step function input to the bipolar amplifier which drives the coil, to apply a step torque in time to the free end of the specimen. The specimen was allowed to stabilize for at least two days within the apparatus before creep testing was begun, to allow recovery from any prior loads to occur. Creep compliance was calculated from the measured torque, M, angular displacement, $\phi(t)$ as a function of time t, specimen radius, r, and length, L, using the quasistatic relation:

$$J(t) = \frac{\phi(t) 0.5 \pi r^4}{ML}. \tag{1}$$

In dynamic (sinusoidal) experiments, the stiffness was considered as the absolute value of the complex shear modulus G^*. At frequencies significantly below that of the specimen's first torsional resonance, G^* was approximated by the quasistatic relation between moment M^*, length L, radius r, and twist angle ϕ:

$$|G^*| = \frac{M^* L}{\phi(0.5 \pi r^4)}. \tag{2}$$

Damping, expressed as the phase δ between stress and strain, was calculated in the subresonant domain using the lumped relation between the material phase δ and the measured phase φ between torque and angular displacement:

$$\tan \delta = \tan \varphi [1 - (\nu/\nu_0)^2], \tag{3}$$

where ν is the frequency at which the data are measured, and ν_0 is the resonant frequency. At frequencies well below any resonance,

$$\tan \delta \approx \tan \varphi. \tag{4}$$

Coupling with flexural modes has not been a problem with this apparatus. Such coupling manifests itself as a weak spurious resonance at intermediate frequencies below the first torsional mode, and was observed in the 50Sn50Pb specimen. Data near the subresonance were masked, leaving a small gap in the data. Such effects were minimized by making the specimen and the end attachment as symmetrical as possible.

For materials of comparatively low loss at frequencies corresponding to a resonant torsional or bending resonant mode of the specimen, damping was calculated using the shape of the frequency response curve near the resonance (the resonance half-width method):

$$\tan \delta \approx \frac{\Delta \nu}{\nu_0 \sqrt{3}}, \tag{5}$$

where $\Delta\omega$ is the full width of the resonance curve at half maximum. A related approach using the width at $1/\sqrt{2}$ of maximum is valid within 1% for $\tan \delta \leqslant 0.28$.[4]

III. RESULTS

Dynamic and creep results for 80In15Pb5Ag at −6, 21, and 50 °C, and some dynamic results at −11 °C are shown in Fig. 2. The normalized stiffness and tan δ are plotted versus

frequency. At the small strain used in the study, the alloys exhibit linear viscoelasticity rather than the viscoplasticity observed by others at larger strain. The stiffness was normalized to a frequency of 1 Hz and a temperature of 21 °C, at which the shear modulus was measured as 5.2 GPa. Creep data versus time t were plotted on the same graph as dynamic (sinusoidal) data versus frequency ν using the relation[5] $\nu = 1/2\pi t$.

Dynamic and creep results for 50Sn50Pb at 21 °C are shown in Fig. 3, which shows normalized stiffness and tan δ plotted versus frequency. The stiffness was normalized to a frequency of 1 Hz and a temperature of 21 °C, at which the shear modulus was 9.1 GPa. Figure 3 also shows results by Brodt, Cook, and Lakes for 52In48Sn for comparison. Also plotted in Fig. 3 is tan δ versus frequency for 63Sn37Pb, an alloy similar to 50Sn50Pb, measured by Woirgard, Sarrazin, and Chaumet.[6] Woirgard *et al.* noted a small knee in the tan δ curve for 63Sn37Pb at 0.1 Hz, but they did not provide a detailed description of their 63Sn37Pb specimen. A similar small knee in the tan δ curve was also observed for 50Sn50Pb at 0.05 Hz. The tan δ measured for 50Sn50Pb is approximately 4.4 times that reported by Woirgard *et al.* for 63Sn37Pb in the frequency range of 10^{-4}–10^{-2} Hz, and 3.5 times that reported by Woirgard *et al.* in the frequency range from 0.1 to 10 Hz. Another difference between these alloys was found by Steinberg,[7] who reported that the fatigue life for 63Sn37Pb is twice as long for 50Sn50Pb in reversed shear and four times as long for reversed bending. Steinberg reported fatigue data for several tin/lead alloys, and in all cases, the higher the lead content, the lower the fatigue life. This indicates that tin/lead alloys behave differently based on the composition, so the difference seen here in the damping is not inconsistent with differences seen in fatigue. Also, damping in metals is affected by grain structure and dislocation density, which depends on cold work. Wire specimens tend to be heavily cold worked.

The solder alloys exhibit much more creep and damping than structural metals such as steel, brass, and aluminum alloys, for which tan δ can range from 10^{-3} to less than 10^{-5}.

IV. CAUSAL MECHANISMS

It is generally agreed that the high-temperature background (which refers to the rapid increase in the damping of metals when the temperature is above about half of the homologous temperature) is caused by a combination of thermally activated dislocation mechanisms. Viscoelasticity rather than viscoplasticity is observed at the small strains used in this study, since the strain is too small to cause dislocation breakaway, which gives rise to plastic deformation. The solders, having low melting temperatures, are at high homologous temperature at room temperature. Most prior experimental studies which disclosed high-temperature background have been focused primarily on other damping mechanisms such as grain boundary slip or the Zener mechanism for atomic movement in alloys; the high-temperature background was superposed on the phenomenon of primary interest. Also, in most prior experiments temperature has

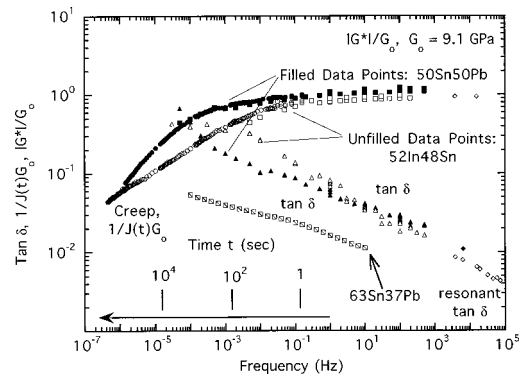

FIG. 3. Stiffness and tan δ vs frequency for wire 50Sn50Pb and cast 52In48Sn at 21 °C (shear modulus, $G_0 = 9.1$ GPa for 50Sn50Pb at 1 Hz, 21 °C). Tan δ vs frequency for 63Sn37Pb following Woirgard *et al.* shown for comparison.

been scanned rather than frequency since it is easier to do so. Schoeck, Bisogni, and Shyne[8] supposed a generic thermally activated dislocation point defect mechanism and arrived at an expression for the dependence of the background mechanical damping tan δ on absolute temperature T and angular frequency $\omega = 2\pi\nu$:

$$\tan\delta = \frac{K}{[\omega \exp(U_0/kT)]^n}, \tag{6}$$

in which K is a constant, k is Boltzmann's constant, and U_0 is the activation energy of the rate-controlling process, and n is a constant. This equation describes an Arrhenius-type temperature dependence of properties, with a modified activation energy. The true activation energy, U, is thought to be related to the rate-controlling activation energy, U_0, by $U = nU_0$. For example, the activation energy for vacancy motion can range from 10% to 30% of the self-diffusion activation energy for some body-centered-cubic (bcc) metals, and from 40% to 60% for face-centered-cubic (fcc) metals.[9] Depending on the reference, indium is reported to be bcc,[10] tetragonally deformed fcc,[11] or face-centered tetragonal.[12] Lead is fcc[1] and silver is fcc.

The activation energy, 55.4 kJ/mol, of the rate-controlling process was inferred from the shift in the creep curves with temperature as presented below. Behavior was thermorheologically simple over at least nine decades of true time and frequency, which means a change in temperature was equivalent to a shift of viscoelastic property curves versus log time or log frequency. The dominant causal mechanisms responsible for behavior over nine decades of true time and frequency therefore have the same temperature sensitivity. A single causal mechanism may be operative over the full range of time and frequency.

Diffusion data for indium, lead, and silver are shown in Table I. The values are from the *CRC Handbook of Chemistry and Physics*,[13] unless otherwise noted (Refs. 19 and 20 in Table I). These data suggest that the deformation mechanism for viscoelastic behavior of this particular alloy is governed by lattice diffusion of silver in indium, which has an activation energy of 48 and 54 kJ/mol depending on direction. Referring to Table I, the diffusion coefficient, D_T, is given

TABLE I. Diffusion data for silver, lead, and indium.

Solute	Matrix	Activation energy (kJ/mol)	Frequency factor, D_0 (cm^2/s)
Silver	Indium	$S\perp c$ 53.5, $S\parallel c$ 48.1	$S\perp c$ 0.52, $S\parallel c$ 0.11
Lead	Indium	Not Available	Not Available
Indium	Indium	$S\perp c$ 78.2, $S\parallel c$ 78.2	$S\perp c$ 3.7, $S\parallel c$ 2.7
Silver	Lead	P 60.2, 63.5[a]	P 14.4, 15.2
Lead	Lead	S 106.9, 106.7,[b] 109.2, 103.7	S 0.887, 0.88, 1.4, 0.7
Indium	Lead	Not Available	Not Available
Silver	Silver	S 189.4	S 0.67
Lead	Silver	P 159	P 0.22
Indium	Silver	S 171	S 0.41

S: Single crystal, P: polycrystalline, $\perp c$: perpendicular to c direction, $\parallel c$: parallel to c direction.
[a]Reference 19.
[b]Reference 20.

by an Arrhenius equation, $D_T = D_0 \exp\{-U/RT\}$ in which D_T is the diffusion coefficient, D_0 is the frequency factor, U is the activation energy, $R = 8.31$ J/mol, K is the gas constant, and T is the absolute temperature. A variety of viscoelastic mechanisms, including dislocation drag, may be governed by an underlying diffusion process, therefore identification of an activation energy does not permit identification of a particular mechanism in this case.

As for PbSn, since experimental data are available at only one temperature, one cannot infer the activation energy. However, observe that the activation energy for lattice self-diffusion[14] of tin in tin is 105–107 kJ/mol depending on crystallographic direction, and for lead in lead, 107–109 kJ/mol.

As for more specific understanding of the viscoelastic mechanism, Eq. (6) does not allow one to predict the exponent of the observed power-law frequency dependence of $\tan\delta = A\nu^{-\beta}$ about 0.001 Hz. Here β is identical to n in Eq. (6). Experimentally, the $\tan\delta$ levels off at low frequency rather than increasing without bound. The dislocation drag model expressed in Eq. (6) assumes no restoring force on the dislocation; the version incorporating a restoring force predicts $\tan\delta$ to decrease at sufficiently low frequency. Such a decrease was not seen in this study or in experiments over eleven decades on eutectic In–Sn.[15] Moreover, a self-organized criticality dislocation model which predicts $\beta = 2$ for all materials was excluded by measurements showing $\beta < 1$ over many decades of frequency in several eutectic and γ-phase In–Sn alloys.[15] As presented below, $\beta < 1$ is also obtained for the alloys examined in the present study. The behavior is not consistent with the Deybe form:

$$\tan\delta = \Delta \frac{\omega\tau}{1+\omega^2\tau^2}, \tag{7}$$

with τ as a relaxation time and $\omega = 2\pi\nu$.

Deybe peaks cover about one decade of frequency and at frequencies well above the Deybe peak, $\tan\delta \propto \nu^{-1}$. Many relaxation mechanisms, including order-disorder processes, thermoelastic relaxation, and Zener relaxation in solid solutions,[1] give rise to a Debye peak.

V. CONSTITUTIVE MODELING

A. 80In15Pb5Ag

The following normalized, dimensionless constitutive equation was used to model the dependence of the creep compliance of these alloys on time t (in sec) and absolute temperature T (in K). It consists of a sum of a stretched exponential form and a power law in time

$$J(t,T) = J_0[1 - \hat{A} e^{-[t/\tau_r(T)]^\beta}] + \{t/\tau_c(T)\}^m, \tag{8}$$

with $0 < \beta \leq 1$ as the stretched exponent, and J_0 and $\hat{A}$ as constants. $\tau_r(T)$ is a characteristic retardation time, and $\tau_c(T)$ is a characteristic time for creep. The temperature dependence is assumed to be Arrhenius: $\tau_r^{-1} = \tau_{r0}^{-1} \exp\{-U/RT\}$ and $\tau_c^{-1} = \tau_{c0}^{-1} \exp\{-U/RT\}$. The normalizing shear modulus is $G_0 = 5.2$ GPa. Two terms are used rather than one owing to the large range of frequency studied (nine decades).

Since overall curve fitting of creep is much more sensitive to the second term than the first term, the stretched exponent β was determined from $\tan\delta$ versus frequency above 0.001 Hz as shown in Fig. 4. To use the creep compliance model given in Eq. (8) for dynamic $\tan\delta$ which depends on frequency ν, the dynamic data were converted to time depen-

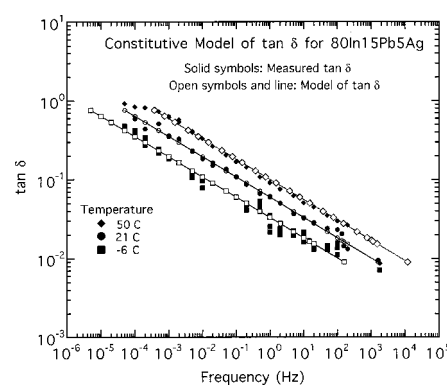

FIG. 4. Comparison of experimental results and shifted $\tan\delta$ based on time-temperature superposition model for 80In15Pb5Ag at −6, 21, and 50 °C.

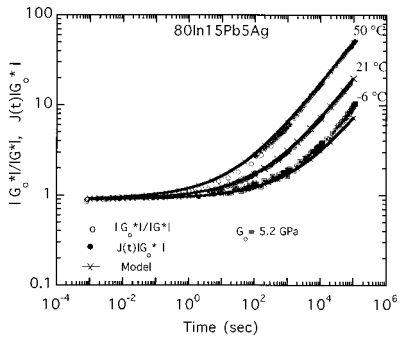

FIG. 5. Comparison of creep and dynamic modulus results and the creep compliance model for 80In15Pb5Ag at −6, 21, and 50 °C.

dent creep data, using $\nu = 1/2\pi t$. In this portion of the curve, tan δ is related to frequency based on the following equation:

$$\tan\delta = A\nu^{-\beta}, \tag{9}$$

in which tan δ is mechanical damping and A and β are constants. The slope β for frequencies is the same stretched exponent as in Eq. (8), well above the peak in tan δ from the first term, as can be demonstrated numerically. However, an analytical interrelation between creep $J(t)$ and damping tan δ is not available for general values of β. Values for the stretched exponent, β, and constant, A, at temperatures of −6, 21, and 50 °C, were determined by curve fitting. Within the 95% confidence interval, β is independent of temperature. A stretched exponent $\beta = 0.257$, determined by averaging the calculated value of β over temperature, was used in the overall constitutive model of 80In15Pb5Ag. The 95% confidence interval in the stretched exponent, β was ±0.010 at 21 and 50 °C, ±0.015 at −6 °C, and ±0.030 at −11 °C. This aspect of the modeling deals with frequencies above about 0.001 Hz; it represents neither the rolloff in damping at lower frequency nor creep. Experimental results for tan δ for −6, 21, and 50 °C are compared in Fig. 4 with tan δ shifted according to the thermally activated model.

The parameters, J_0, $\hat{A}$, and m as well as the activation energy U in Eq. (8) for $J(t,T)$ were determined by curve fitting for −6, 21, and 50 °C over the full nine decades of creep and dynamic compliance data. For all temperatures, $J_0 = 1.043$, $\hat{A} = 0.147$, $\beta = 0.257$, $m = 0.487$, $U = 55.44$ kJ/mol K. Time parameters were $\tau_{r0} = 5.60 \times 10^{-10}$ s, with $\tau_{c0} = 3.37 \times 10^{-8}$ s. The correlation coefficients for the models were 0.999 or better at 21 and at 50 °C, and 0.998 at −6 °C. The poorer fit at −6 °C is attributed to convection-induced noise during cooling. Experimental and modeled creep and equivalent dynamic compliance results are plotted in Fig. 5 for −6, 21, and 50 °C.

Therefore, the alloy is thermorheologically simple. Plazek[16] has pointed out that given data within a fairly narrow experimental window (3 decades or less) the test for thermorheological simplicity can only be definitive in its failure. That is, such an experiment is capable of demonstrating thermorheological complexity but it cannot demonstrate simplicity. Plazek showed that nearly perfect superposition was obtained for data for polystyrene over a restricted range of 3.4 decades, but that data over 6 decades could not be superposed. It is notable that the alloy considered here is thermorheologically simple over nine decades of true frequency. The temperature range −6–50 °C gives a shift of about 1.9 decades of effective time or frequency.

TABLE II. Parameters used in creep compliance model [Eq. (8)] for 50Sn50Pb.

Model Parameter	50Sn50Pb, 21 °C	80In15Pb5Ag, 21 °C
J_0	1.024	1.043
$\hat{A}$	0.151	0.147
β	0.167	0.257
τ_r(s)	1.0	4.08
m	0.560	0.478
Correlation coefficient, R	0.999362	0.999960
G_0(GPa), 1 Hz	9.1	5.2
95% confidence interval for β	±0.006	±0.010

The sensitivity of the model was checked by varying the model parameters one at a time by ±10%. The remaining parameters were held constant. The model is most sensitive to the power law stress exponent, m. It is less sensitive to the other parameters. A change in the characteristic times causes a shift of the creep curve versus log time; while a change in the power law stress exponent, m, causes a change in slope of the creep portion of the curve.

B. 50Sn50Pb. Comparisons

Since data for 50Sn50Pb were measured at one temperature, 21 °C the constitutive parameters obtained apply to that temperature. As done above, the constants in the creep compliance model [Eq. (8)], specifically the stretched exponent, β, and constant, $\hat{A}$, for 50Sn50Pb were determined at 21 °C. These and other model parameters are listed in Table II. Corresponding values for 80In15Pb5Ag at 21 °C are also listed. The values for the two solders are compared at the same operational temperature, not the same homologous temperature.

Creep compliance versus time curve on a logarithmic scale has slope $m = 0.560$ for 50Sn50Pb, higher than 0.478 for 80In15Pb5Ag, so more creep takes place in a given decade for 50Sn50Pb than 80In15Pb5Ag.

Tan δ at higher frequencies followed the $\nu^{-\beta}$ dependence of Eq. (9). For 50Sn50Pb, $\beta = 0.167$. Experimental and modeled tan δ for 50Sn50Pb at 21 °C are compared in Fig. 6,

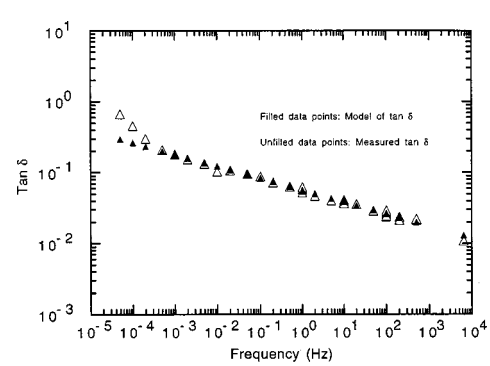

FIG. 6. Comparison of experimental results and tan δ model for 50Sn50Pb.

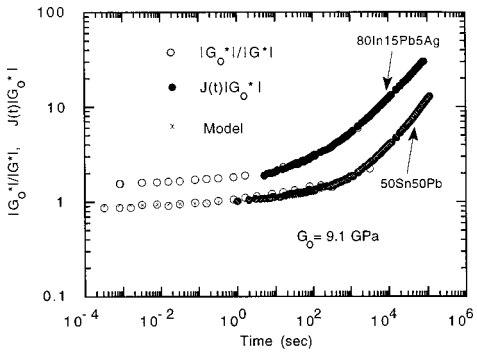

FIG. 7. Comparison of experimental results and the creep compliance model for 50Sn50Pb at 21 °C and 80In15Pb5Ag at 21 °C, both normalized to $G_0 = 9.1$ GPa.

and a similar comparison for creep compliance $J(t)$ is plotted in Fig. 7. The parameters J_0 and B are normalized using $G_0 = 9.1$ GPa.

The stretched exponent, β, is the slope of the tan δ versus frequency curve on a logarithmic scale for frequencies well above the damping peak in the stretched exponential portion of the model. The stretched exponent for 50Sn50Pb is 0.167, compared to 0.257 for 80In15Pb5Ag. Because of this difference in slope, the tan δ for 50Sn50Pb is higher than that of 80In15Pb5Ag above 1 Hz, and lower than that of 80In15Pb5Ag at frequencies below 1 Hz. Other alloys such as InSn, SnCd, and SnSb also exhibited tan δ which approximately followed a $\nu^{-\beta}$ dependence over a range of frequency. Deviations from this pattern may be in the form of peaks; if so they are poorly defined. The value of β was 0.17 for SnCd and 0.12 for SnSb,[17] compared with 0.28 for InSn[17] and 0.32 for InBi, 0.27 for InCd and 0.44 for InSnCd.[18]

The same technique used to develop these viscoelastic models could be extended to the viscoplastic, nonisothermal conditions that are commonly experienced during thermal cycling by the solder joints in electronic assemblies.

VI. CONCLUSIONS

Tan δ followed a $\nu^{-\beta}$ dependence over many decades of frequency for these alloys. Results for 80In15Pb5Ag are consistent with a creep function consisting of a stretched exponential combined with a power law in the time domain and an Arrhenius dependence on temperature. Behavior was thermorheologically simple over at least nine decades of true time and frequency.

[1] A. S. Nowick and B. S. Berry, *Anelastic Relaxation in Crystalline Solids* (Academic, New York, 1972), pp. 435–462.
[2] M. Brodt, L. S. Cook, and R. S. Lakes, Rev. Sci. Instrum. **66**, 5292 (1995).
[3] W. G. Gottenberg and R. M. Christensen, Int. J. Eng. Sci. **2**, 45 (1965).
[4] E. J. Graesser and C. R. Wong, in *M^3D: Mechanics and Mechanisms of Material Damping*, edited by V. K. Kinra and A. Wolfenden (ASTM, Philadelphia, 1992).
[5] R. S. Lakes, *Viscoelastic Solids* (CRC, Boca Raton, FL, 1999).
[6] J. Woirgard, Y. Sarrazin, and H. Chaumet, Rev. Sci. Instrum. **48**, 1322 (1977).
[7] D. S. Steinberg, *Vibration Analysis for Electronic Equipment*, 2nd ed. (Wiley, New York, 1988).
[8] G. Schoeck, E. Bisogni, and J. Shyne, Acta Metall. **12**, 1466 (1964).
[9] Y.-H. Pao, S. Badgley, E. Jih, R. Govila, and J. Browning, J. Electron. Packag. **115**, 147 (1993).
[10] R. P. Reed, C. N. McCowan, J. D. McColskey, R. P. Walsh, L. A. Delgado, C. Brady, M. W. Austin, and S. A. Kim, *Low-Temperature Properties of Indium, Final Report-Phase I* (Fracture and Deformation Division, D. E. Newbury, Gas and Particulate Science Division, National Bureau of Standards, Boulder, Colorado 80303, 1987).
[11] C. L. Vold, M. E. Glicksman, E. W. Kammer, and L. C. Cardinal, J. Phys. Chem. Solids **38**, 157 (1977).
[12] *Constitution of Binary Alloys*, edited by M. Hansen (McGraw–Hill, New York, 1958).
[13] *CRC Handbook of Chemistry and Physics*, 68th ed., Editor-in-Chief, R. C. Weast, Ph.D., Associate Editors, M. J. Astle, Ph.D., and W. H. Beyer, Ph.D. (CRC, Boca Raton, FL, 1987–1988).
[14] R. Darveaux, and K. Banerji, IEEE Trans. Compon., Hybrids, Manuf. Technol. **15**, 1013 (1992).
[15] R. S. Lakes and J. Quackenbush, Philos. Mag. Lett. **74**, 227 (1996).
[16] D. J. Plazek, J. Rheol. **40**, 987 (1996).
[17] J. Quackenbush and R. S. Lakes, Scr. Metall. Mater. **35**, 441 (1996).
[18] M. Brodt and R. S. Lakes, J. Mater. Sci. **31**, 6577 (1996).
[19] *Diffusion in Solids, Recent Developments*, edited by A. S. Nowick and J. J. Burton (Academic, New York, 1975).
[20] S. K. Sen and A. Ghorai, Philos. Mag. A **59**, 707 (1989).